Mikada, H., Moore, G.F., Taira, A., Becker, K., Moore, J.C., and Klaus, A. (Eds.)
Proceedings of the Ocean Drilling Program, Scientific Results Volume 190/196

5. Data Report: Normalization Factors for Semiquantitative X-Ray Diffraction Analysis, with Application to DSDP Site 297, Shikoku Basin[1]

Michael B. Underwood,[2] Nandini Basu,[2] Joan Steurer,[2] and Swati Udas[2]

ABSTRACT

This data report documents the acquisition of two new sets of normalization factors for semiquantitative X-ray diffraction analyses. One set of factors is for bulk sediment powders, and the other applies to oriented aggregates of clay-sized fractions (<2 µm). We analyzed mixtures of standard minerals with known weight percentages of each component and solved for the normalization factors using matrix singular value decomposition. The components in bulk powders include total clay minerals (a mixture of smectite, illite, and chlorite), quartz, plagioclase, and calcite. For clay-sized fractions, the minerals are smectite, illite, chlorite, and quartz. We tested the utility of the method by analyzing natural mudstone specimens from Site 297 of the Deep Sea Drilling Project, which is located in the Shikoku Basin south of Site 1177 of the Ocean Drilling Program (Ashizuri transect).

INTRODUCTION

Analysis of sediment samples by X-ray diffraction (XRD) has been a routine part of shipboard and shore-based measurements by the Ocean Drilling Program (ODP) and the Deep Sea Drilling Project (DSDP). The presence of specific detrital and/or authigenic minerals can be detected

[1]Underwood, M.B., Basu, N., Steurer, J., and Udas, S., 2003. Data report: Normalization factors for semiquantitative X-ray diffraction analysis, with application to DSDP Site 297, Shikoku Basin. *In* Mikada, H., Moore, G.F., Taira, A., Becker, K., Moore, J.C., and Klaus, A. (Eds.), *Proc. ODP, Sci. Results,* 190/196, 1–28 [Online]. Available from World Wide Web: <http://www-odp.tamu.edu/publications/190196SR/VOLUME/CHAPTERS/203.PDF>. [Cited YYYY-MM-DD]
[2]Department of Geological Sciences, University of Missouri, Columbia MO 65211, USA. Correspondence author: **UnderwoodM@missouri.edu**

Initial receipt: 4 November 2002
Acceptance: 6 June 2003
Web publication: 22 August 2003
Ms 190SR-203

easily through visual recognition of characteristic peak positions. It is more difficult, however, to estimate the relative abundance of a mineral with meaningful accuracy (Moore, 1968; Cook et al., 1975; Heath and Pisias, 1979; Johnson et al., 1985; Mascle et al., 1988). Fisher and Underwood (1995) developed a method during ODP Leg 156 to calculate abundances of common minerals in bulk powders using matrix singular value decomposition (SVD). They derived normalization factors based on the peak areas of diagnostic XRD reflections, as produced by standard mineral mixtures with known weight percentages of each component. In essence, this method accounts for changes in any given mineral's peak dimensions as a function of its own absolute abundance, as well as the abundance of every other mineral in the mixture.

When the method of Fisher and Underwood (1995) is applied to natural samples of marine sediment, the accuracy of absolute weight percent values deteriorates as additional minerals and amorphous solids (e.g., volcanic glass and biogenic silica) increase in number and amount. Consequently, the mineral percentages calculated by SVD are relative only with respect to the other minerals in the standard mixtures (e.g., weight percent quartz relative to total clay, plagioclase, and calcite). In the case of diatomaceous ooze or vitric mud, this limitation could lead to substantial errors in estimates of absolute mineral abundance relative to all solid phases. Another limitation of the SVD approach is the need to establish sets of normalization factors that match each indigenous mineral mixture within each study area. In other words, factors for a kaolinite-rich mineral suite from Barbados or Costa Rica will not work for an illite-chlorite assemblage in Nankai Trough or Cascadia. Thus, some advanced knowledge of the natural sediment's composition is a prerequisite to mixing appropriate mineral standards. A third significant limitation is imposed by design differences in X-ray diffractometers (e.g., a fixed-step vs. continuous-scan mode, or automatic vs. fixed slits). Separate normalization factors are needed for each type of instrument. This requirement is especially important if there is a desire to integrate shipboard and shore-based data sets generated by different instruments. A final consideration is the individual instrument performance (e.g., life span of X-ray tube and detector). If peak intensities change significantly with tube life, recalibration may be warranted.

Similar questions of accuracy arise during the semiquantitative calculations of clay mineral percentages. The most common approach in marine geology is to apply the Biscaye (1965) peak area weighting factors during calculations of the relative proportions of smectite, illite, and chlorite. The errors in such data can be substantial, however, and they change with the absolute abundance by weight of each mineral (Underwood et al., 1993). Results can also shift because of interlaboratory differences in sample disaggregation and chemical treatments, particle size separation, and the degree of preferred orientation of clay mounts (Moore and Reynolds, 1989; McManus, 1991). Even though the reproducibility of such data might be good, the typical estimates of accuracy are no better than ±10%.

The purpose of this data report is to document the acquisition of new normalization factors for analyses of bulk powder and clay-sized mixtures in sediments from the Nankai Trough and Shikoku Basin (Fig. **F1**). Recalibration of the methodology was required for several reasons: (1) to allow accurate comparisons among bulk powder data generated by shipboard (Philips) and shore-based (Scintag) XRD systems; (2) to improve mergers of data from DSDP Site 297 and ODP Leg 190; (3) to improve the accuracy of calculated relative mineral percentages within the

F1. Location map, p. 9.

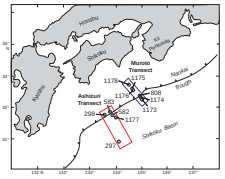

clay-sized fraction (<2 µm); and (4) to improve the accuracy of calculated percentages of specific clay minerals (e.g., weight percent smectite) within the bulk sediment. We also include the results of bulk powder and clay-fraction analyses of samples from DSDP Site 297 to illustrate fully the utility of the method. The data from Site 297 are important for characterizing the composition of subduction inputs within the Ashizuri transect of Nankai Trough (Fig. F1), and they have been used to document how frictional properties change as a function of total clay content and clay mineralogy (Brown et al., in press).

METHODS/MATERIALS

Standard Mineral Mixtures

The mineral standards used for the new bulk powder mixtures are similar to those used during ODP Leg 190: quartz (St. Peter sandstone), feldspar (Ca-rich albite), calcite (Cyprus chalk), illite (2M1 polytype), and chlorite. We discovered that the specimen of Wyoming montmorillonite (Swy-2) used during Leg 190 contains an unacceptable amount of contamination (mostly by quartz); it was replaced by a relatively pure smectite (Ca-montmorillonite). We also decided to omit kaolinite (Clay Mineral Society Kga-1) from the mixtures because its abundance in Nankai sediments at Site 808 is only 8%–20% of the kaolinite + chlorite clay-sized fraction (Orr, 1992), which amounts to <3% of the typical bulk sediment. Table T1 shows the percentages by dry weight of each mineral in the 14 mixtures that we analyzed.

T1. Bulk-powder mixtures, p. 19.

The standards used for the clay-sized mixtures are smectite (Ca-montmorillonite), illite (Clay Mineral Society Imt-2), chlorite (Clay Mineral Society Cca-2), and quartz (St. Peter sandstone). We included quartz in the mix because of the desire to quantify the nonclay component of the clay-sized fraction in natural specimens and for correcting peak positions relative to quartz (100). Each standard was powdered thoroughly using a Spex Certiprep 5100 mixer mill, suspended in ~500 mL of distilled water with sodium hexametaphosphate dispersant, and disaggregated using an ultrasonic cell disrupter. Particles <2 µm equivalent settling diameter were separated by centrifugation (1000 rpm for 2.4 min; ~320× g). The purity of each clay-sized separate was confirmed by XRD. The average concentration of each suspension was determined by extracting and drying three aliquots at 75°C to obtain dry weight of clay per unit volume of suspension, corrected for weight of dispersant. The weights for smectite probably reflect a hydration state containing two layers of interlayer water. Volumetric proportions of the four components were measured by pipette, then converted to dry weights and weight percentages. Table T2 shows the percentages by dry weight of each mineral in the mixtures that we analyzed. Mixture 7 is nearly pure smectite and was not included in the calculation of normalization factors.

T2. Clay-sized mineral mixtures, p. 20.

Sample Preparation

Bulk samples of natural sediment were freeze-dried, hand crushed by mortar and pestle, and powdered for 5 min using a Spex Certiprep 5100 mixer mill. The standard mineral mixtures were also run through the mixer mill for 5 min to improve their homogenization. The bulk powders were then packed gently into XRD sample holders to retain ran-

dom orientation. The mixtures of standard minerals were analyzed three times each and remixed between each run using the ball mill.

Isolation of clay-sized fractions started with drying and gentle crushing of the mud/mudstone, after which specimens were immersed in 3% H_2O_2 for at least 24 hr to digest organic matter. We then added ~250 mL of sodium hexametaphosphate solution (concentration = 4 g/1000 mL) and inserted beakers into an ultrasonic bath for several minutes to promote disaggregation and deflocculation. This step (and additional soaking) was repeated for highly indurated samples until visual inspection indicated complete disaggregation. Washing consisted of two passes through a centrifuge (8200 rpm for 25 min; ~6000× g), with resuspension in distilled water after each pass. After transferring the suspended sediment to a 60-mL plastic bottle, each sample was resuspended by vigorous shaking and a 2-min application of a sonic cell probe. The clay-sized fractions (<2 µm equivalent settling diameter) then were separated by centrifugation (1000 rpm for 2.4 min; ~320× g). Oriented aggregates of natural samples and standard clay mixtures were prepared using the filter-peel method and 0.45-µm membranes (Moore and Reynolds, 1989). Three separate slides were prepared for each of the standard clay mixtures. The clay aggregates were saturated with ethylene glycol for at least 24 hr prior to XRD analysis, using a closed vapor chamber heated to 60°C in an oven.

X-Ray Diffraction Parameters

The XRD laboratory at the University of Missouri utilizes a Scintag Pad V X-ray diffractometer with CuK_α radiation (1.54 Å) and a Ni filter. Scans of bulk powders were run at 40 kV and 35 mA over a scanning range of 3° to 35°2θ at a rate of 1°2θ/min and a step size of 0.01°2θ. Scans of oriented clay aggregates were run at 40 kV and 30 mA over a scanning range of 2° to 23°2θ, a rate of 1°2θ/min, and a step size of 0.01°2θ. Slits were 0.5 mm (divergence) and 0.2 mm (receiving). We processed the digital data using MacDiff software (version 4.2.5) to establish a baseline of intensity, smooth counts, correct peak positions (relative to quartz), and calculate peak intensities and peak areas.

Figure F2 shows the resulting diffractograms for the bulk powder mineral mixtures. Normalization factors were established for the integrated areas of the following peaks: composite clay mineral at ~19.8°2θ (d-value = 4.49 Å); quartz (101) at 26.65°2θ (d-value = 3.34 Å); a characteristic double peak for plagioclase at 27.77°–28.02°2θ (d-value = 3.21–3.18 Å); and calcite (104) at 29.42°2θ (d-value = 3.04 Å). We did not record the dimensions of individual clay mineral peaks generated by bulk powders because of low intensities and interference between smectite (001) and chlorite (001) reflections.

Figure F3 shows the resulting diffractograms for the clay-sized mineral mixtures. The normalization factors for clay aggregates are based on the integrated areas of a broad smectite (001) peak centered at around 5.3°2θ (d-value = 16.5 Å), the illite (001) peak at 8.93°2θ (d-value = 9.9 Å), the chlorite (002) peak at 12.53°2θ (d-value = 7.06 Å), and the quartz (100) peak at 20.95°2θ (d-value = 4.24 Å).

F2. Standard mineral mixtures analyzed as random bulk powders, p. 10.

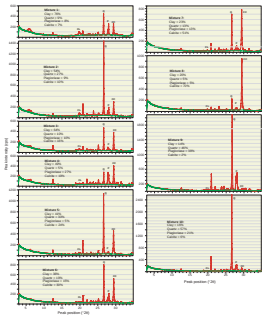

F3. Standard mineral mixtures analyzed as oriented clay aggregates, p. 12.

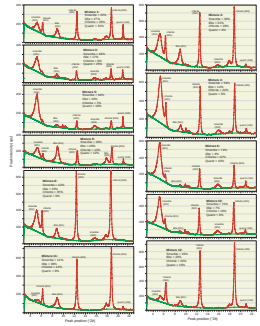

RESULTS

Bulk Powder Standards

The results of XRD analyses of the bulk powder standards are shown in Table T3. Diagnostic peak areas increase in a fairly consistent manner as a function of that mineral's absolute abundance by weight (Fig. F4). To reduce the effects of heterogeneity among the three batches of standards, we used the average values of peak area to calculate the normalization factors shown in Table T4. Table T3 also lists the calculated values of relative weight percent for each component in each mineral mixture, as well as the error of each value relative to the measured weight. The errors for total clay are the largest (average = 3%), but with one exception are 5% or less. Errors for plagioclase are the smallest (average = 1%). The errors associated with the shore-based standards are smaller, on average, than those produced during shipboard measurements (Shipboard Scientific Party, 2001), and they are more consistent in size. The shipboard errors average 4% for clay, 3% for quartz, and 2% for plagioclase and calcite. Contamination of the smectite standard and peak interference between chlorite and kaolinite contributed to those larger and more erratic errors.

Comparison with Shipboard Results

Because of our desire to compare shore-based and shipboard data with confidence, we selected a suite of specimens to reanalyze at the University of Missouri. Table T5 shows the samples selected, the new XRD peak areas, and the calculated mineral abundances. Roughly one-half of the reruns were completed on exactly the same bulk powder that was analyzed shipboard, but the others utilized adjacent intervals within sampling "clusters" that may have extended 5 to 10 cm up and down a core. In addition, during the shipboard calculations of total clay, we added together the individual responses of clay peaks generated by four clay minerals, whereas shore-based calculations relied on a single composite peak. Neither approach is without flaw because the intensity of the composite peak depends on both total clay and which specific clay mineral is most abundant. The differences in methodology, as expected, led to systematic shifts in calculated mineral abundances for the natural sediments (Fig. F5). Results from the *JOIDES Resolution* (Moore, Taira, Klaus, et al., 2001) shift total clay and plagioclase lower (by an average of 6 and 4 wt%, respectively) as compared to shore-based replicates. Replicates shift values of calcite and quartz higher for shipboard data by an average of 2 and 8 wt%, respectively.

Clay Mineral Standards

The results of XRD analyses of the clay-sized standards are shown in Table T6. As with the bulk powders, linear regression shows that the diagnostic peak areas increase in a fairly consistent manner as a function of each mineral's absolute abundance (Fig. F4). Because of heterogeneity among the three batches of oriented clay aggregates, we used the average values of peak area to calculate the normalization factors shown in Table T4. Table T6 also lists the calculated values of relative weight percent for each component of each mineral mixture, as well as the error for each value relative to the true measured weight. The errors for

T3. XRD results for bulk powder mixtures, p. 21.

F4. Measured weight percent vs. average peak area from XRD, p. 13.

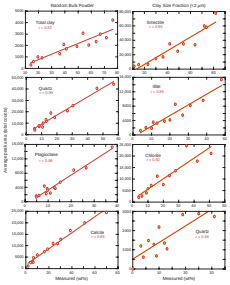

T4. Normalization factors for bulk powers and clay-sized aggregates, p. 22.

T5. Shore-based vs. shipboard XRD values, p. 23.

F5. Replicate analyses of random bulk powders, p. 14.

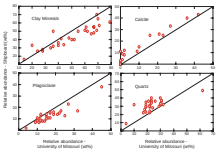

T6. XRD data and error analysis for clay-sized standards, p. 24.

smectite are the largest (maximum = 5%; average = 3%). Errors for illite are 2% or less, and those for chlorite are 3% or less.

Table T6 also lists normalized percentages for clay minerals only (i.e., %smectite + %illite + %chlorite = 100%). These data permit direct comparisons with values calculated using the Biscaye (1965) peak area weighting factors: 1× for smectite (001) peak area, 4× for illite (001), and 2× for chlorite (002). The errors using SVD are no greater than 5% and are typically less than 4%, with no systematic shifts. The Biscaye peak area method, conversely, consistently underestimates by 7% to 17% the amount of smectite by weight. Overestimates of illite are as high as 16 wt% using Biscaye (1965) for the standards, and the calculated values for chlorite are typically 5 to 8 wt% higher than their true weight percentages.

Application of Method to Samples from DSDP Site 297

The new SVD normalization factors have been applied to analyses of both bulk powders and oriented clay-sized aggregates using samples from DSDP Site 297. We characterized their composition as part of a pilot study to show how the coefficient of internal friction and shear strength change within the Shikoku Basin facies (Brown et al., in press). Our results for bulk powders are listed in Table T7. The data for the clay-sized fraction are listed in Table T8.

Figure F6 shows how relative abundances of total clay minerals, quartz, and plagioclase change as a function of stratigraphic position at Site 297. Contents of calcite are trivial, and smear slides show very little biogenic silica. The assemblage of clay minerals (smectite + illite + chlorite) increases in relative abundance toward the bottom of the Lower Shikoku Basin turbidite facies and throughout the volcaniclastic-rich facies. Analyses of the <2-µm size fraction demonstrate that this enrichment of total clay is caused by an increase in smectite. Percentages of smectite by weight within the clay sized fraction are as high as 50%-99%.

The absolute values displayed in Figure F7 are, of course, method-dependent. Figure F8 compares calculations of relative weight percent for each clay mineral using the SVD normalization factors vs. percent by weighted peak area using the Biscaye (1965) weighting factors. Percentages of smectite increase systematically (by as much as 15 to 20 wt%) using the SVD factors, whereas percentages of illite decrease systematically. Values of chlorite change modestly as a function of method. Analysis of error for the standard mineral mixtures (Table T6) indicates that the SVD-based data are more accurate indicators of mineral abundance by weight or volume.

One of the goals of shore-based research associated with ODP Leg 190 is to determine how sediment frictional properties change as a function of mineralogy, especially the abundance of smectite. Another goal is to determine how smectite dehydration affects fluid pressure and fluid flow within and beneath the accretionary prism. The reliability of empirical studies and numerical simulations will improve as our estimates of "absolute" clay-mineral abundance become more accurate. This objective is difficult to achieve using XRD, however, because of the inability to measure abundances of amorphous solids. In addition, the relation between clay in the mineral assemblage and clay in the grain size distribution is complicated. Sand and silt fractions within the trench-wedge and Shikoku Basin facies contain substantial amounts of

T7. XRD data, random bulk powders, Site 297, p. 25.

T8. XRD data, oriented clay-sized fraction, Site 297, p. 26

F6. Random bulk powders from Site 297, p. 15.

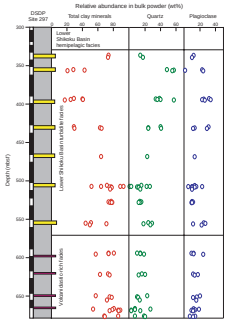

F7. Oriented clay-sized aggregates from Site 297, p. 16.

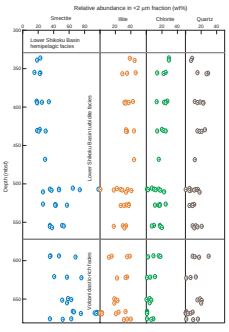

F8. Weighting vs. SVD factors for Site 297, p. 17.

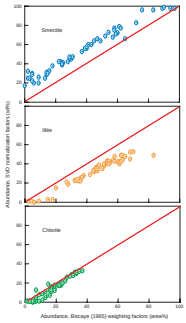

altered volcanic rock fragments, mudstone-shale fragments, detrital mica and chlorite, and low-grade meta-sedimentary fragments (e.g., Fergusson, this volume). Thus, the difference between %clay in the bulk powder and %clay in the clay-sized fraction is impossible to pinpoint. With this caveat in mind, we estimated the amount of each clay mineral in the bulk powder by multiplying the weight percent of total clay by the relative percentage of each clay mineral in the <2-µm size fraction (Fig. F9) (where %smectite + %illite + %chlorite = 100%). Values of weighted peak area based on Biscaye (1965) weighting factors are 5 to 10 wt% lower than those based on SVD, but both sets of data indicate that smectite abundance within the lower Shikoku Basin is typically greater than 30 wt% of the bulk sediment.

F9. Clay mineral abundance in bulk sediments from Site 297, p. 18.

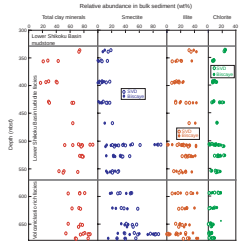

CONCLUSIONS

We assembled a new set of standard mineral mixtures for XRD analysis of bulk powders from Nankai Trough using the SVD method and the Scintag diffractometer at the University of Missouri. The new normalization factors are more accurate than the factors used during shipboard analyses during Leg 190. They result in a systematic increase (by an average of ~6 wt%) in estimates of total clay in bulk powders, whereas values for quartz decrease by an average of 8 wt%. We also assembled a set of standard mineral mixtures for oriented clay-sized aggregates (smectite + illite + chlorite + quartz). Estimates of relative mineral abundance based on SVD normalization factors are considerably more accurate than estimates based on Biscaye (1965) peak area weighting factors. Regardless of which method is used, core samples from DSDP Site 297 show significant increases of smectite within the lower part of the Shikoku Basin. Percentages of smectite within the bulk sediment are typically >30 wt% within the lower part of the turbidite facies and within the volcaniclastic-rich facies.

ACKNOWLEDGMENTS

We thank the crew, technicians, and fellow scientists aboard the *JOIDES Resolution* for their assistance with sample acquisition during Leg 190. Andy Fisher kindly employed his code for matrix singular value decomposition to calculate new sets of normalization factors. Arpit Ghoting and Anup Bidesi assisted with sample preparation. We thank Dawn Cardace for her review of the manuscript. This project utilized samples provided by the Ocean Drilling Program (ODP). The ODP is sponsored by the U.S. National Science Foundation (NSF) and participating countries under management of Joint Oceanographic Institutions (JOI), Inc. Funding was provided by the U.S. Science Support Program (grant F001281 to Underwood) and a Schlanger Ocean Drilling Fellowship to Steurer.

REFERENCES

Biscaye, P.E., 1965. Mineralogy and sedimentation of recent deep-sea clays in the Atlantic Ocean and adjacent seas and oceans. *Geol. Soc. Am. Bull.,* 76:803–832.

Brown, K.M., Kopf, A., Underwood, M.B., and Weinberger, J.L., in press. Compositional and fluid pressure controls on the state of stress on the Nankai subduction thrust. *Earth Planet. Sci. Lett.*

Cook, H.E., Johnson, P.D., Matti, J.C., and Zemmels, I., 1975. Methods of sample preparation and X-ray diffraction data analysis, X-ray Mineralogy Laboratory, Deep Sea Drilling Project, University of California, Riverside. *In* Hayes, D.E., Frakes, L.A., et al., *Init. Repts. DSDP,* 28: Washington (U.S. Govt. Printing Office), 999–1007.

Fisher, A.T., and Underwood, M.B., 1995. Calibration of an X-ray diffraction method to determine relative mineral abundances in bulk powders using matrix singular value decomposition: a test from the Barbados accretionary complex. *In* Shipley, T.H., Ogawa, Y., Blum, P., et al., *Proc. ODP, Init. Repts.,* 156: College Station, TX (Ocean Drilling Program), 29–37.

Heath, G.R., and Pisias, N.G., 1979. A method for the quantitative estimation of clay minerals in North Pacific deep-sea sediments. *Clays Clay Miner.,* 27:175–184.

Johnson, L.J., Chu, C.H., and Hussey, G.A., 1985. Quantitative clay mineral analysis using simultaneous linear equations. *Clays Clay Miner.,* 33:107–117.

Mascle, A., Moore, J.C., Taylor, E., and Shipboard Scientific Party, 1988. ODP Leg 110 at the northern Barbados Ridge: introduction and explanatory notes. *In* Mascle, A., Moore, J.C., et al., *Proc. ODP, Init. Repts.,* 110: College Station, TX (Ocean Drilling Program), 5–25.

McManus, D.A., 1991. Suggestions for authors whose manuscripts include quantitative clay mineral analysis by X-ray-diffraction. *Mar. Geol.,* 98:1–5.

Moore, C.A., 1968. Quantitative analysis of naturally occurring multicomponent mineral systems by X-ray diffraction. *Clays Clay Miner.,* 16:325–336.

Moore, D.M., and Reynolds, R.C., Jr., 1989. *X-ray Diffraction and the Identification and Analysis of Clay Minerals:* Oxford (Oxford Univ. Press).

Moore, G.F., Taira, A., Klaus, A., et al., 2001. *Proc. ODP, Init. Repts.,* 190 [CD-ROM]. Available from: Ocean Drilling Program, Texas A&M University, College Station TX 77845-9547, USA.

Orr, R.M., 1992. Clay mineralogy, diagenesis, and provenance of sediments in the Nankai Trough, offshore Shikoku Island, southwest Japan [M.S. thesis]. Univ. of Missouri, Columbia.

Shipboard Scientific Party, 2001. Explanatory notes. *In* Moore, G.F., Taira, A., Klaus, A., et al., *Proc. ODP, Init. Repts.,* 190, 1–51 [CD-ROM]. Available from: Ocean Drilling Program, Texas A&M University, College Station TX 77845-9547, USA.

Underwood, M.B., Orr, R., Pickering, K., and Taira, A., 1993. Provenance and dispersal patterns of sediments in the turbidite wedge of Nankai Trough. *In* Hill, I.A., Taira, A., Firth, J.V., et al., *Proc. ODP, Sci. Results,* 131: College Station, TX (Ocean Drilling Program), 15–34.

Figure F1. Map showing locations of DSDP (Deep Sea Drilling Project) and ODP (Ocean Drilling Program) sites along the northern edge of Shikoku Basin and Nankai Trough, Philippine Sea.

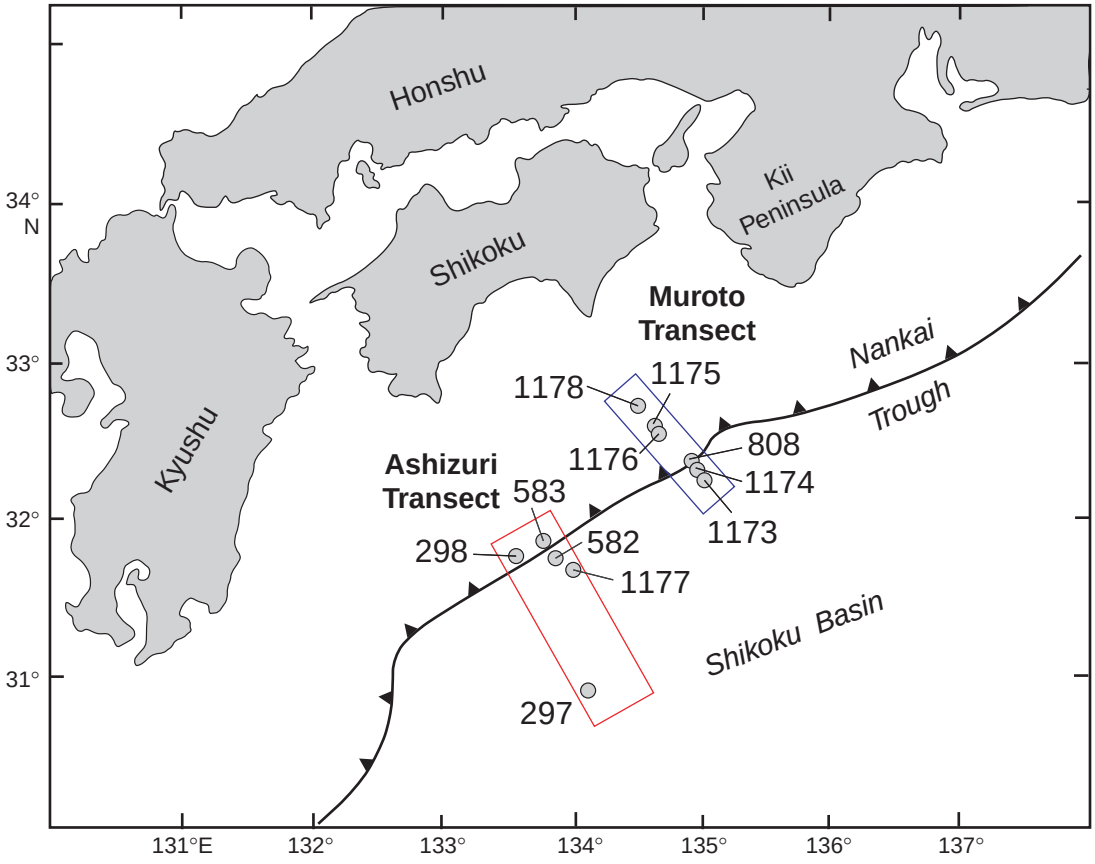

Figure F2. X-ray diffractograms for standard mineral mixtures analyzed as random bulk powders. Note the actual weight percentages of each mineral within each mixture. Peaks used for calculation of SVD (singular value decomposition) normalization factors are labeled as follows: CL = composite clay minerals, Q = quartz, P = plagioclase, CC = calcite. (Continued on next page.)

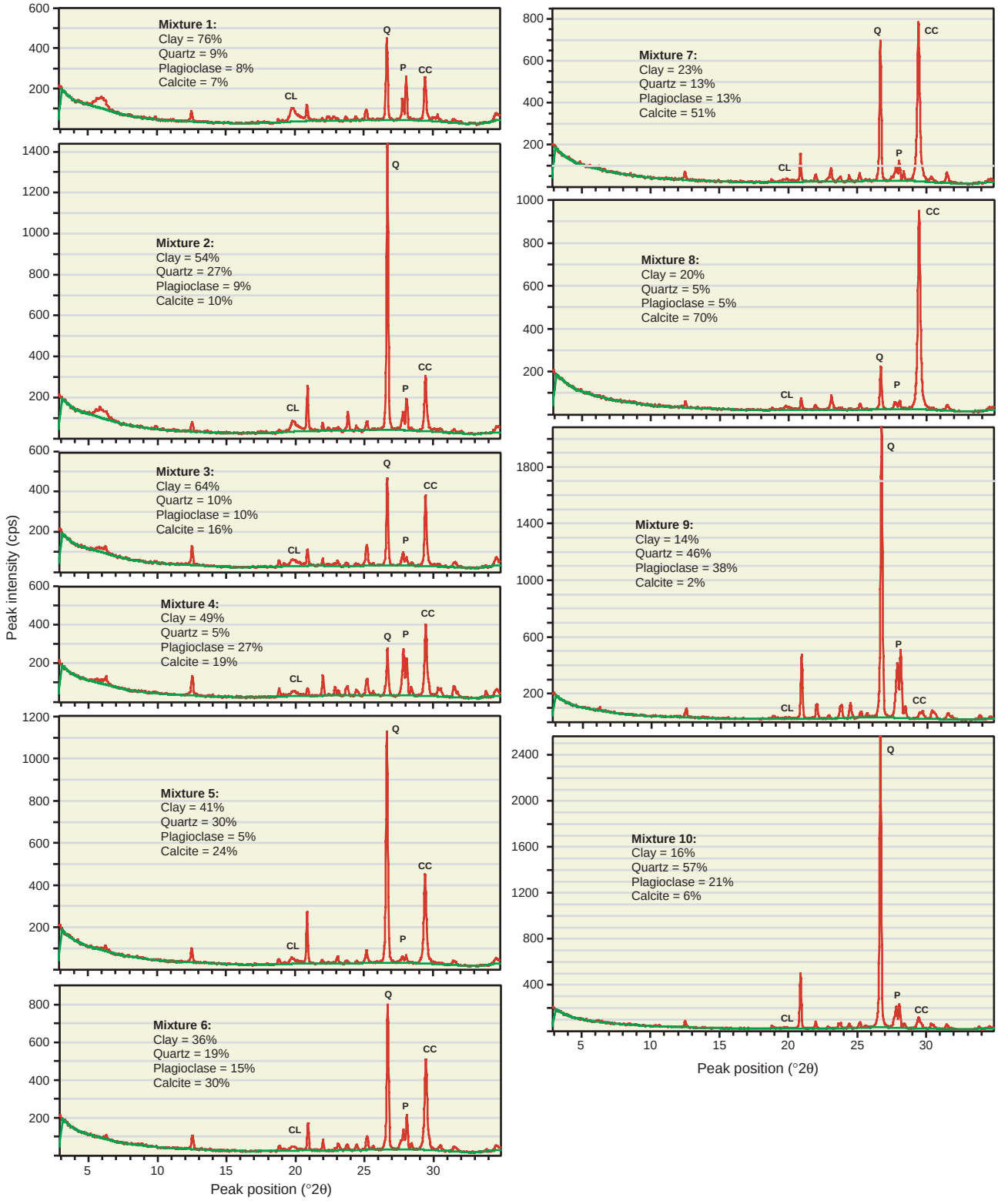

Figure F2 (continued).

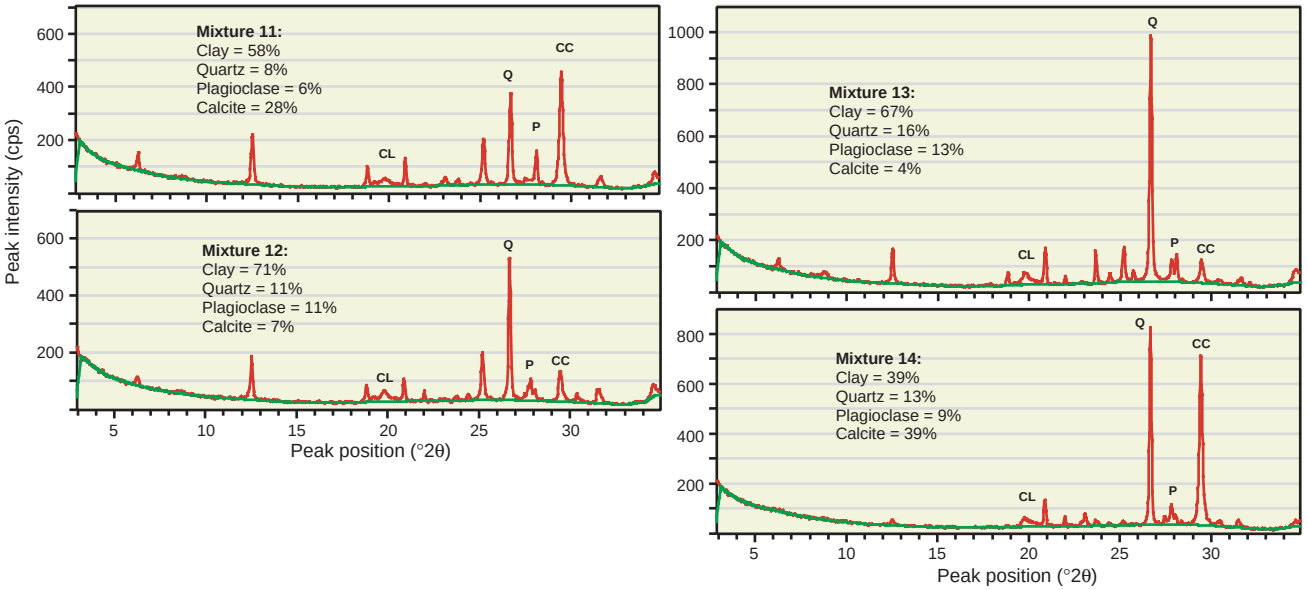

Figure F3. X-ray diffractograms for standard mineral mixtures analyzed as oriented clay aggregates (<2 µm). Note the actual weight percentages of each mineral within each mixture. Peaks used for calculation of SVD (singular value decomposition) normalization factors are smectite (001), illite (001), chlorite (002), and quartz (100).

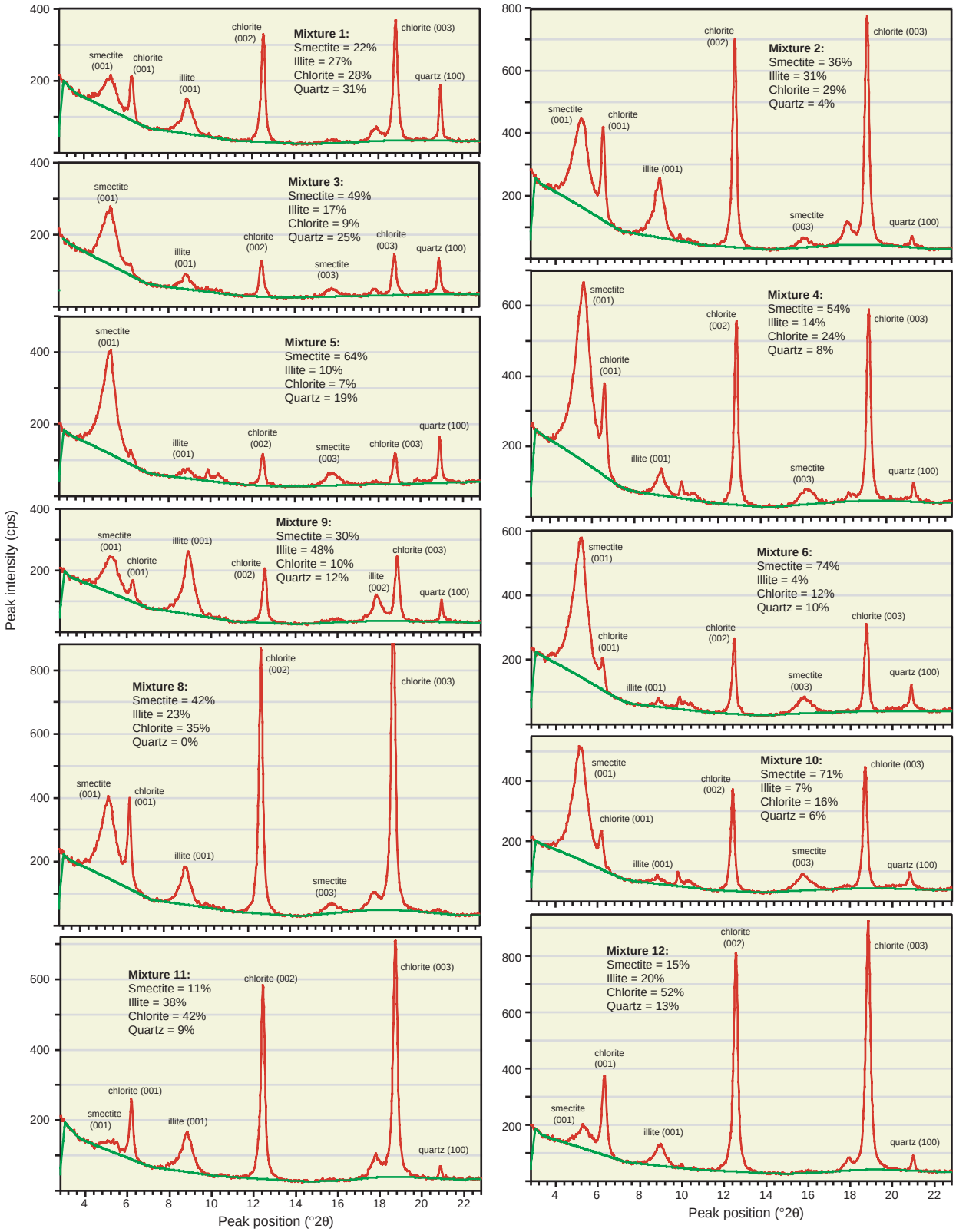

Figure F4. Linear regression plots of measured weight percent vs. average peak area from X-ray diffraction. Plots on the left show results for random bulk powders (see Fig. F2, p. 10, for diffractograms). Plots on the right show results for oriented clay-sized aggregates (see Fig. F3, p. 12, for diffractograms). Correlation coefficients are shown as r-values. See Tables T3, p. 21, and T6, p. 24, for error analysis.

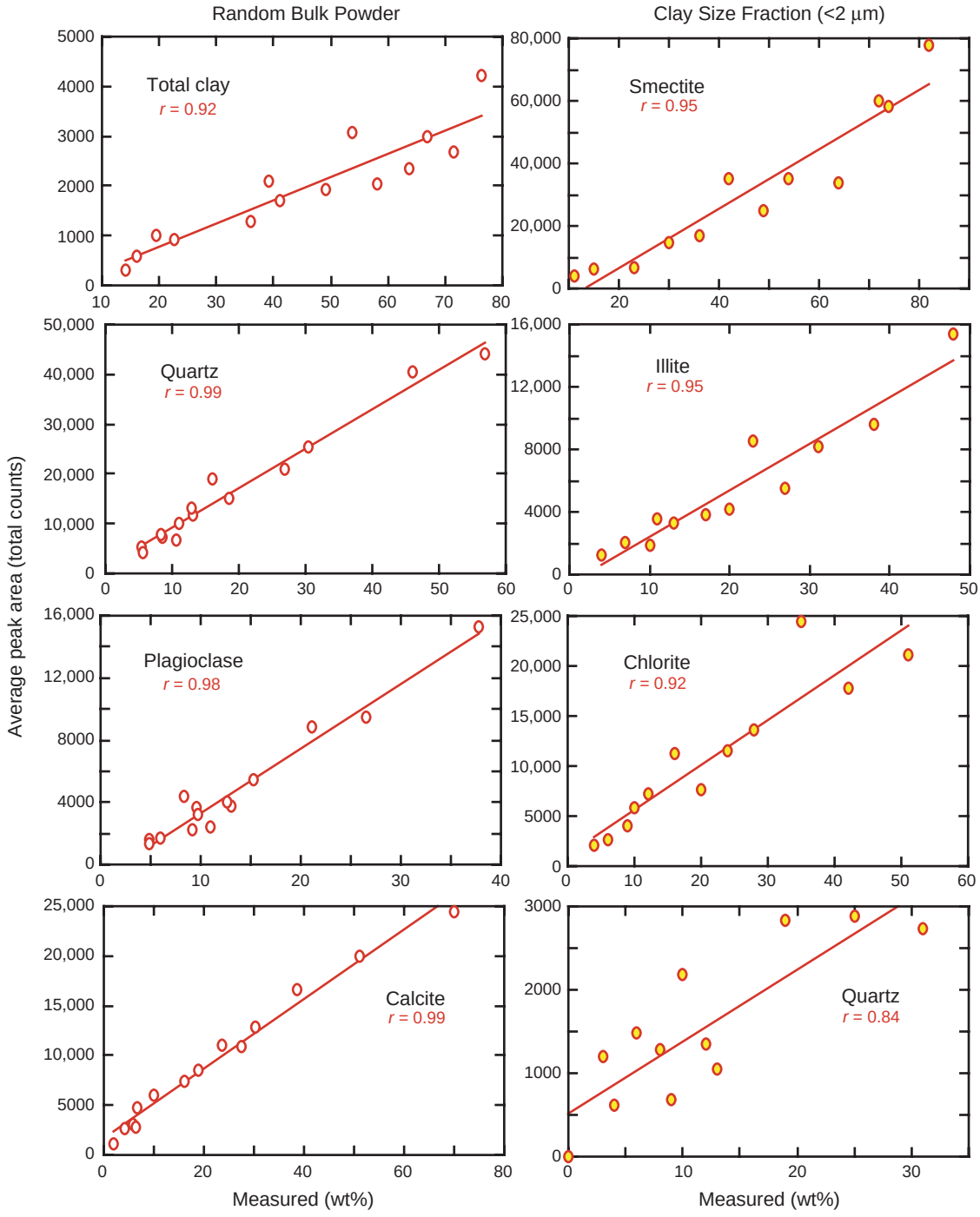

Figure F5. Results of replicate analyses of random bulk powders measured on the *JOIDES Resolution* and at the University of Missouri. Values of relative abundance (in weight percent) are based on the SVD (singular value decomposition) method (Fisher and Underwood, 1995) but utilize different sets of normalization factors. Reference lines correspond to 1:1 match. See Table T5, p. 23, for tabulated data.

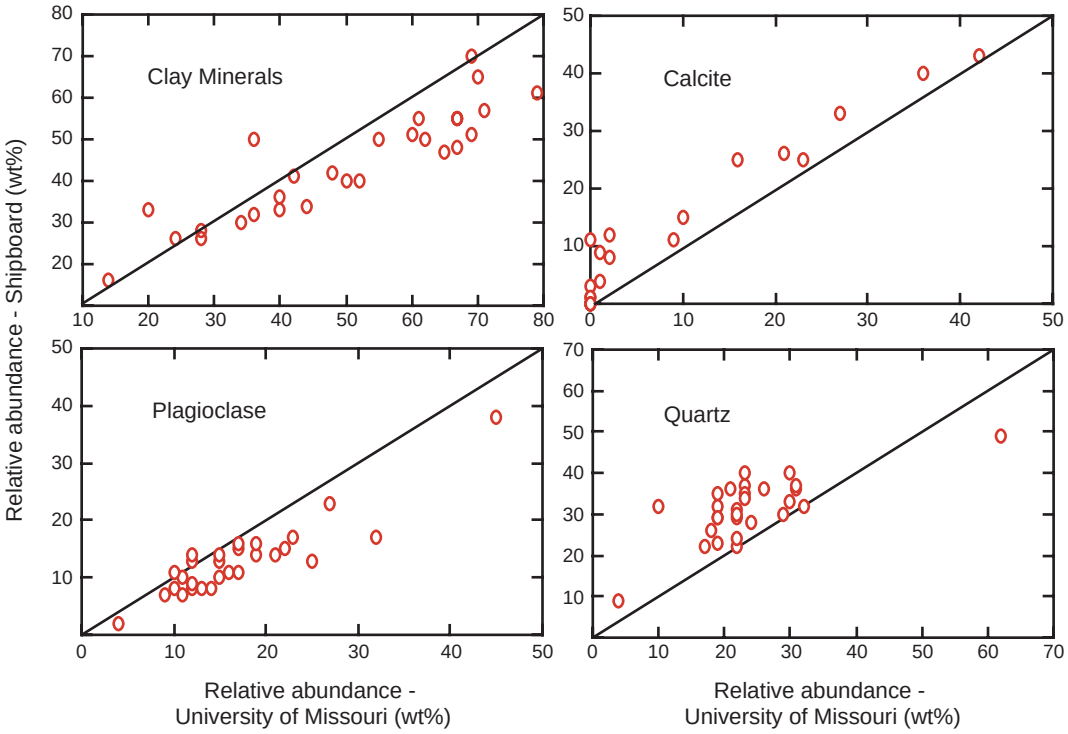

Figure F6. Results of X-ray diffraction analysis of random bulk powders from Site 297 of the Deep Sea Drilling Project. Data are tabulated in Table T7, p. 25. See Figure F1, p. 9, for location. Cored intervals are indicated in white to the left of stratigraphic column; intervals that were drilled ahead are indicated in black. Values of relative abundance (in weight percent) are based on the SVD (singular value decomposition) method using normalization factors shown in Table T4, p. 22.

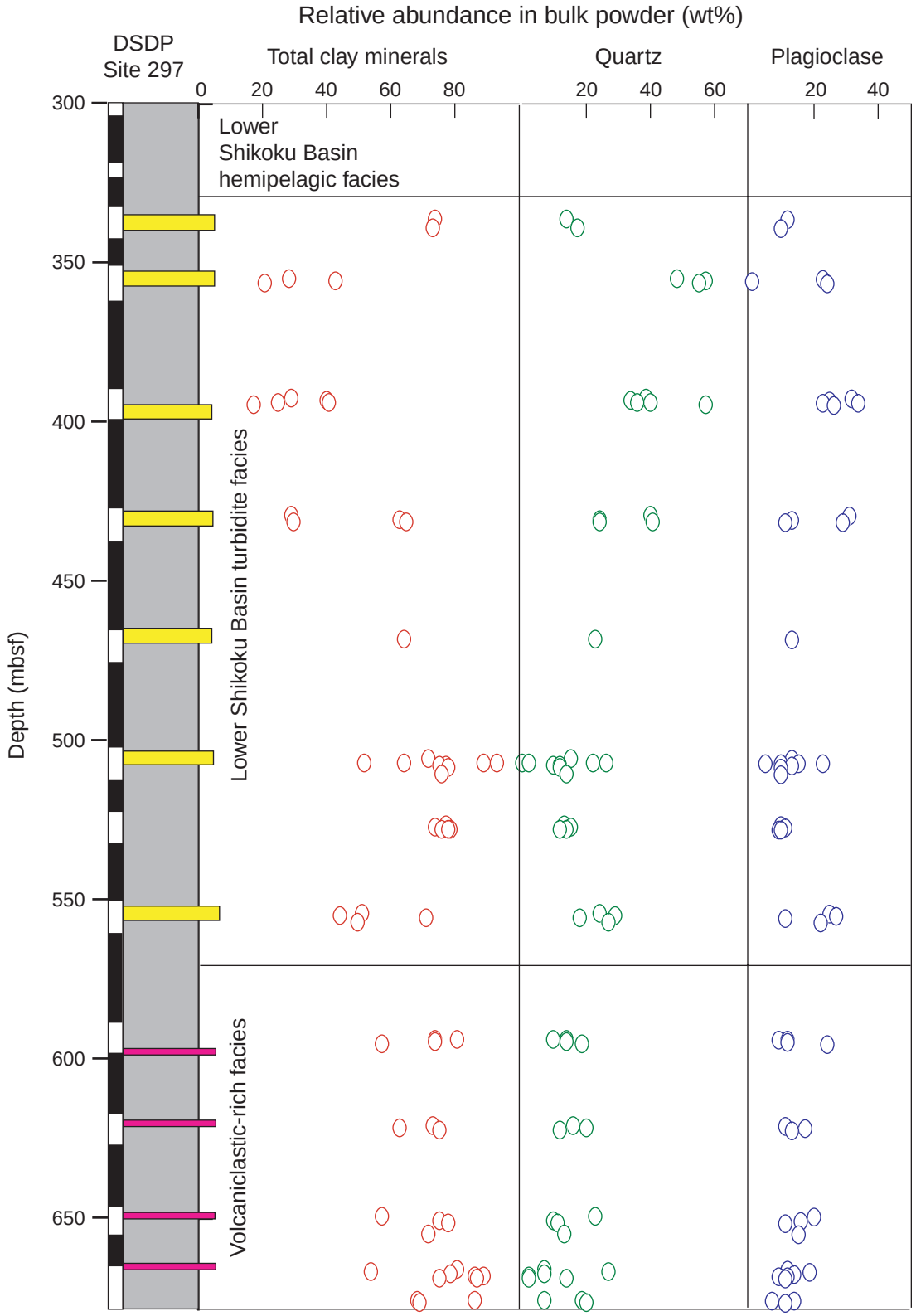

Figure F7. Results of X-ray diffraction analysis of oriented clay-sized aggregates from Site 297 of the Deep Sea Drilling Project. Data are tabulated in Table T8, p. 26. See Figure F1, p. 9, for location and Figure F6, p. 15, for stratigraphic column. Values of relative abundance (in weight percent) are based on the SVD (singular value decomposition) method using normalization factors shown in Table T4, p. 22.

Figure F8. Comparison of relative clay mineral abundance for DSDP samples from Site 297 using Biscaye (1965) weighting factors and SVD (singular value decomposition) normalization factors (Table **T4,** p. 22). See Table **T6,** p. 24, for error analysis.

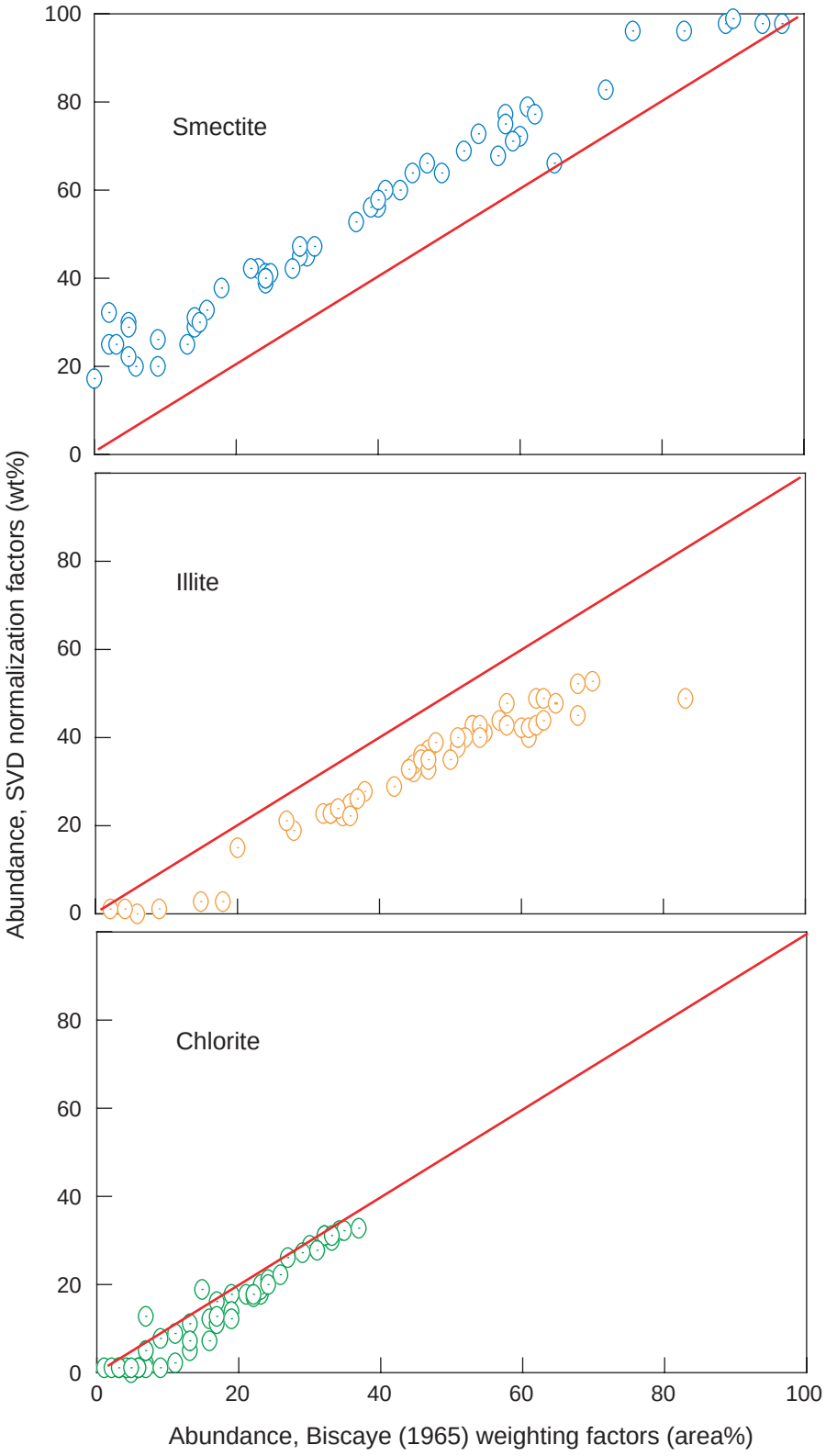

Figure F9. Calculated values of clay mineral abundance within bulk sediment samples from DSDP Site 297. See Figure F1, p. 9, for location and Figure F6, p. 15, for stratigraphic column. Percentages of total clay minerals are based on X-ray diffraction analyses of random bulk powders (Table T7, p. 25). Estimates of the percentage contributed by each individual clay mineral are products of total clay (Table T7, p. 25) times the relative percentage of each clay within the <2-µm size fraction (where %smectite + %illite + %chlorite = 100%) (Table T8, p. 26). Open circles = estimates derived from SVD (singular value decomposition) method, solid circles = values based on Biscaye (1965) weighting factors.

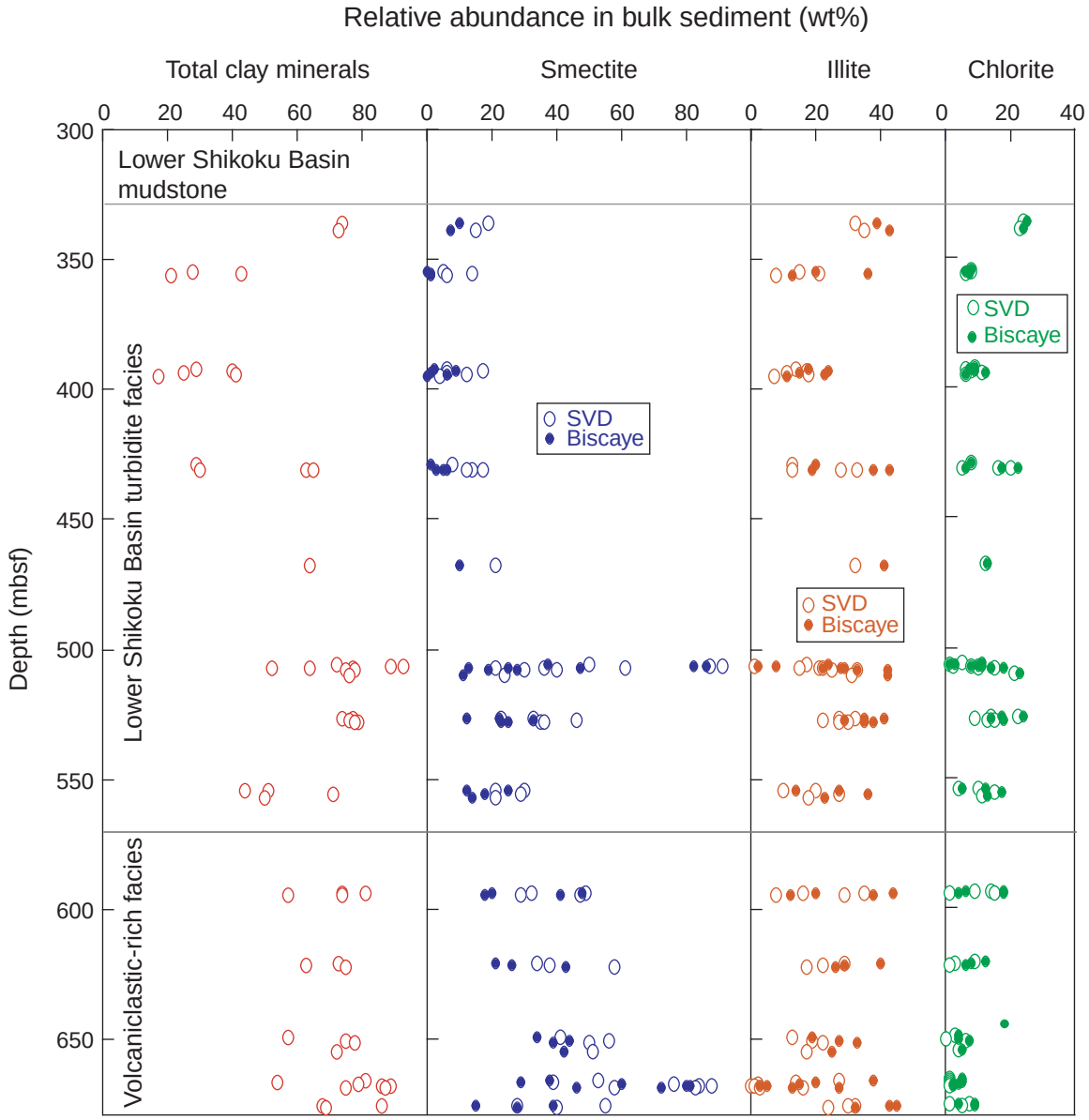

Table T1. Bulk-powder mixtures for calibration of normalization factors

Mix	Target minerals (wt%)						
	Smectite	Illite	Chlorite	Total clay	Quartz	Plagioclase	Calcite
1	58	9	10	76	9	8	7
2	39	7	8	54	27	10	10
3	34	6	24	64	11	10	16
4	25	5	20	49	6	27	19
5	19	9	13	41	31	5	24
6	10	13	13	36	19	15	30
7	7	6	10	23	13	13	51
8	6	8	6	20	6	5	70
9	8	0	6	14	46	38	2
10	0	8	9	16	57	21	6
11	9	20	30	58	8	6	27
12	12	26	33	71	11	11	7
13	14	33	20	67	16	13	4
14	20	15	4	39	13	9	39

Table T2. Clay-sized (<2 µm) mineral mixtures for calibration of normalization factors.

	Target minerals (wt%)			
Mix	Smectite	Illite	Chlorite	Quartz
1	22	27	20	31
2	36	31	29	4
3	49	17	9	25
4	54	14	24	8
5	64	10	7	19
6	74	4	12	10
8	42	23	35	0
9	30	48	10	12
10	71	7	16	6
11	11	38	42	9
12	15	20	52	13

Table T3. X-ray diffraction results for bulk powder standard mixtures.

	Peak intensity (cps)				Peak area (total counts)				Calculated abundance (wt%)				Error (calculated – measured) (%)			
Mix	Total clay	Quartz	Plagioclase	Calcite	Total clay	Quartz	Plagioclase	Calcite	Total clay	Quartz	Plagioclase	Calcite	Total clay	Quartz	Plagioclase	Calcite
1	68	413	190	210	4,226	7,404	4,365	4,690	77	6	11	6	1	–3	3	–1
2	50	1,264	106	264	3,075	21,015	3,652	6,062	59	22	9	10	5	–5	–1	0
3	34	404	140	341	2,361	6,718	3,209	7,340	61	9	11	20	–3	–2	1	4
4	27	333	268	369	1,926	5,387	9,478	8,550	47	5	26	21	–2	–1	–1	2
5	28	1,491	38	428	1,710	25,426	1,591	11,105	36	31	5	27	–5	1	0	4
6	23	870	181	478	1,280	14,961	5,437	12,820	31	19	16	34	–5	0	1	4
7	15	717	135	777	935	11,746	3,779	20,015	22	14	12	52	–1	1	–1	1
8	17	241	40	927	1,020	4,166	1,349	24,470	22	5	7	66	2	–1	2	–4
9	7	2,343	431	44	322	40,605	15,254	1,183	15	47	37	1	1	1	–1	–1
10	11	2,578	271	96	600	44,193	8,872	3,070	17	55	23	5	1	–2	2	–1
11	30	449	68	419	2,042	7,907	1,678	10,891	51	11	7	31	–7	3	1	4
12	38	531	72	111	2,684	9,932	2,418	2,849	73	14	9	5	2	3	–2	–2
13	47	962	121	94	2,982	19,127	4,063	2,656	64	22	11	2	–3	6	–2	–2
14	38	789	76	673	2,091	13,021	2,283	16,598	41	14	7	38	2	1	–2	–1

Table T4. Normalization factors for X-ray diffraction analysis of random bulk powers and oriented clay-sized aggregates.

Random bulk powders		Affected mineral in standard mixture			
		Total clay	Quartz	Plagioclase	Calcite
Influencing mineral:	Total clay	2.0718E–02	–3.6067E–04	2.4613E–04	–1.3475E–03
	Quartz	–3.8644E–05	1.2340E–03	–2.1509E–05	–6.8407E–05
	Plagioclase	6.6736E–04	–1.2044E–04	2.5357E–03	5.1954E–05
	Calcite	1.1920E–05	1.9068E–05	1.1882E–04	2.7128E–03
<2 µm fraction		Affected mineral in standard mixture			
		Smectite	Illite	Chlorite	Quartz
Influencing mineral:	Smectite	1.0890E–03	–1.5328E–04	–2.4315E–04	–2.1743E–04
	Illite	4.5487E–04	2.9373E–03	–3.3780E–04	9.7609E–06
	Chlorite	1.9984E–05	2.9901E–04	2.2389E–03	2.3975E–04
	Quartz	6.6121E–03	3.3672E–03	3.5400E–03	1.0007E–02

Table T5. Results of shore-based X-ray diffraction for samples on *JOIDES Resolution*.

Core, section, interval (cm)	Peak area (total counts)				Relative mineral abundance (wt%)			
	Total clay	Quartz	Plagioclase	Calcite	Total clay	Quartz	Plagioclase	Calcite
190-1173A-								
64X-5, 58–59	3,145	18,788	3,336	0	69	22	9	0
65X-1, 4–5	658	3,441	383	29,030	14	4	4	77
190-1174A-								
8H-4, 133–134	551	22,479	15,012	0	24	31	45	0
190-1174B-								
32R-5, 130–131	1,267	17,131	7,317	8,507	34	22	22	23
65R-4, 78–80	2,561	18,336	5,080	0	62	23	15	0
70R-2, 98–99	2,428	18,448	4,988	4,947	55	22	14	9
86R-2, 117–119	3,254	20,484	4,213	0	67	23	11	0
190-1175A-								
4H-4, 139–141	1,016	13,814	4,071	2,771	42	29	19	10
9H-6, 146–147	1,194	13,987	4,431	8,300	36	22	16	27
18H-3, 140–142	1,038	12,520	3,612	14,040	28	17	13	42
23X-4, 91–92	935	12,341	4,864	11,010	28	19	17	36
37X-5, 136–138	1,668	24,008	7,986	2,065	44	31	23	2
38X-2, 116–118	1,276	25,622	11,863	363	36	32	32	Trace
39X-2, 100–102	1,844	22,709	7,265	917	48	30	21	Trace
190-1176A-								
14H-4, 132–135	1,453	16,861	4,535	7,519	40	24	15	21
35X-1, 29–30	729	44,381	6,170	997	20	62	17	Trace
190-1177A-								
5R-1, 35–36	930	7,226	4,494	887	52	19	27	2
17R-2, 26–28	3,005	18,906	3,690	0	67	23	10	0
19R-4, 116–118	2,671	13,622	3,693	1,827	69	19	12	1
31R-1, 17–19	3,597	17,927	4,187	0	71	19	10	0
33R-1, 88–90	3,238	21,599	4,935	0	65	23	12	0
37R-3, 34–36	3,205	18,731	4,545	0	67	21	12	0
49R-4, 21–22	4,086	10,930	4,463	0	79	10	11	0
53R-2, 59–60	3,418	16,759	4,656	0	70	18	12	0
190-1178A-								
3H-4, 133–135	1,296	13,233	7,529	5,573	40	19	25	16
11X-4, 124–126	1,746	20,127	6,025	1,669	50	30	19	1
27X-3, 120–122	2,616	17,933	6,088	768	61	22	17	Trace
190-1178B-								
8R-6, 67–70	2,516	20,446	5,237	0	60	26	15	0

Table T6. X-ray diffraction data and error analysis for clay-sized standards.

<2 µm size fraction:

	Peak area (total counts)				Calculated abundance (wt%)*				Error (calculated – measured) (%)*			
Mix	Smectite	Illite	Chlorite	Quartz	Smectite	Illite	Chlorite	Quartz	Smectite	Illite	Chlorite	Quartz
1	6,904	5,537	7,635	2,740	27	25	22	26	4	–2	2	–4
2	17,041	8,172	13,570	623	31	32	30	7	–5	1	1	3
3	24,973	3,839	4,072	2,886	47	18	12	24	–3	1	3	–1
4	35,314	3,250	11,494	1,291	55	13	23	9	0	0	–1	1
5	33,861	1,897	2,599	2,834	59	11	7	23	–5	1	1	3
6	58,195	1,205	7,259	2,176	76	4	9	11	2	0	–2	0
8	34,985	8,494	24,425	0	38	24	38	0	–4	1	3	0
9	14,764	15,412	5,823	1,359	31	48	9	12	2	0	–2	0
10	60,065	2,031	11,199	1,490	76	5	15	5	4	–2	–1	–1
11	4,237	9,622	17,802	692	14	36	39	11	3	–2	–3	1
12	6,086	4,194	21,143	1,047	16	21	48	14	1	1	–3	1

Clay minerals only:

	Relative abundance (wt%)*			Error (calculated – measured) (%)*			Relative abundance (area%)†			Error (calculated – measured) (%)†		
Mix	Smectite	Illite	Chlorite	Smectite	Illite	Chlorite	Smectite	Illite	Chlorite	Smectite	Illite	Chlorite
1	36	34	30	4	–5	1	16	50	34	–17	11	6
2	33	34	32	–4	2	3	22	43	35	–16	10	6
3	61	23	15	–4	1	4	52	32	17	–14	9	5
4	60	15	25	1	0	–1	50	18	32	–9	4	6
5	76	14	9	–4	2	1	73	16	11	–7	4	3
6	85	4	10	3	0	–3	75	6	19	–7	1	6
8	38	24	38	–4	1	3	30	29	41	–12	6	6
9	36	54	10	2	0	–2	17	70	13	–17	16	1
10	79	5	16	3	–2	–1	66	9	25	–10	2	8
11	16	40	44	4	–1	–3	5	49	45	–7	7	–1
12	19	25	56	1	2	–3	9	26	65	–8	2	6

Notes: * = SVD normalization factors. † = Biscaye (1965) weighting factors.

Table T7. X-ray diffraction analysis of random bulk powders, DSDP Site 297.

Core, section, interval (cm)	Depth (mbsf)	Peak area (total counts)				Relative abundance (wt%)			
		Total clay	Quartz	Plagioclase	Calcite	Total clay	Quartz	Plagioclase	Calcite
31-297-									
15-2, 113	336.13	4,211	15,564	5,233	0	74	14	12	0
15-4, 85	338.85	4,131	18,129	4,401	0	73	17	10	0
16-2, 59	354.59	1,460	51,396	11,897	183	28	48	23	Trace
16-2, 130	355.30	1,684	36,802	333	0	43	57	1	0
16-3, 90	356.30	925	54,087	11,503	0	21	55	24	0
17-2, 9	392.09	1,426	45,438	17,522	94	29	39	32	Trace
17-2, 114	393.14	1,790	31,315	10,713	0	40	34	25	0
17-3, 10	393.60	1,334	55,437	22,264	0	25	40	34	0
17-3, 56	394.06	2,329	41,155	12,006	0	41	36	23	0
17-3, 118	394.68	665	55,708	12,789	0	17	57	26	0
18-1, 72	429.22	1,157	37,237	13,302	0	29	40	31	0
18-2, 88	430.88	3,035	21,615	5,043	0	63	24	13	0
18-2, 115	431.15	3,235	21,645	4,434	406	65	24	11	Trace
18-2, 133	431.33	1,199	36,181	12,033	0	30	41	29	0
19-1, 142	467.92	3,164	21,449	5,485	0	64	23	13	0
20-1, 121	505.71	2,608	10,551	3,991	0	72	15	13	0
20-2, 83	506.83	8,740	3,706	7,609	251	89	0	10	Trace
20-2, 90	506.90	8,416	5,376	3,292	0	93	2	5	0
20-2, 112	507.12	3,481	22,341	6,624	0	64	22	15	0
20-2, 119	507.19	3,088	31,029	12,194	0	52	26	23	0
20-3, 4	507.54	5,376	13,772	7,235	994	77	10	13	Trace
20-3, 14	507.64	4,493	14,541	6,064	205	75	12	13	Trace
20-3, 81	508.31	4,491	13,906	4,396	0	78	12	10	0
20-4, 123	510.23	4,342	15,564	4,348	0	76	14	10	0
21-3, 4	526.54	4,554	15,370	4,800	48	77	13	10	Trace
21-3, 36	526.86	3,936	15,477	4,572	0	74	15	11	0
21-3, 112	527.62	4,388	15,746	4,193	0	76	14	9	0
21-3, 125	527.75	4,716	13,635	4,441	0	79	12	10	0
21-3, 129	527.79	5,014	15,368	5,266	0	78	12	10	0
22-2, 67	554.17	2,148	20,634	9,895	0	51	24	25	0
22-2, 110	554.60	2,199	30,275	12,921	0	44	29	27	0
22-3, 79	555.79	3,952	18,647	4,968	0	71	18	11	0
22-4, 49	556.99	2,420	26,059	9,709	0	50	27	22	0
23-3, 76	593.76	5,524	13,629	4,808	0	81	10	9	0
23-3, 100	594.00	3,902	14,281	5,067	0	74	14	12	0
23-4, 0	594.50	4,914	17,930	6,588	0	74	14	12	0
23-4, 43	594.93	4,213	28,729	16,117	189	57	19	24	Trace
24-2, 81	620.81	3,283	13,821	3,865	460	73	16	11	Trace
24-3, 18	621.68	2,427	15,056	5,598	246	63	20	17	Trace
24-3, 86	622.36	3,924	12,475	5,431	0	75	12	13	0
25-2, 109	649.59	2,001	16,103	6,282	0	57	23	20	0
25-3, 64	650.64	1,176	3,168	2,006	0	75	10	16	0
25-3, 121	651.21	1,994	5,717	2,117	0	78	11	11	0
25-6, 66	655.16	1,388	5,138	2,441	0	72	13	15	0
26-1, 27	666.27	4,875	9,815	5,765	271	81	7	12	Trace
26-1, 45	666.45	2,682	26,352	8,214	0	54	27	19	0
26-1, 109	667.09	5,214	10,622	7,157	0	79	7	14	0
26-2, 51	668.01	1,960	1,520	1,552	0	89	2	9	0
26-2, 61	668.11	2,148	1,735	2,401	0	86	2	12	0
26-2, 105	668.55	6,372	5,090	6,331	236	87	2	11	Trace
26-2, 130	668.80	3,922	14,038	4,565	0	75	14	11	0
27-1, 20	675.70	4,295	22,605	7,116	0	68	19	14	0
27-1, 51	676.01	4,877	8,859	2,991	0	86	7	7	0
27-1, 61	676.11	3,559	19,202	4,530	29	69	20	11	Trace

Table T8. X-ray diffraction analysis on oriented clay-sized fraction (<2 µm) DSDP Site 297. (See table notes. Continued on next two pages.)

Core, section, interval (cm)	Depth (mbsf)	Peak area (total counts)				Clay-sized fraction (wt%)*			
		Smectite	Illite	Chlorite	Quartz	Smectite	Illite	Chlorite	Quartz
31-297-									
15-2, 113	336.13	2,718	2,751	3,548	165	23	39	29	8
15-4, 85	338.85	3,504	5,581	6,182	199	19	45	29	7
16-2, 59	354.59	289	12,518	10,544	1,148	15	46	25	15
16-2, 130	355.30	233	2,526	899	852	23	35	14	29
16-3, 90	356.30	353	987	1,069	394	22	29	22	27
17-2, 9	392.09	3,467	8,392	8,518	654	18	43	27	12
17-2, 114	393.14	6,535	4,186	2,431	888	34	34	13	19
17-3, 10	393.60	500	3,143	3,801	881	19	32	25	23
17-3, 56	394.06	6,492	6,758	6,906	990	25	37	23	15
17-3, 118	394.68	774	4,097	4,618	1,091	19	33	25	23
18-1, 72	429.22	1,124	4,265	3,366	1,187	22	34	20	25
18-2, 88	430.88	2,288	8,158	6,464	854	19	44	22	15
18-2, 115	431.15	3,917	6,572	7,520	1,172	21	35	25	18
18-2, 133	431.33	4,293	3,685	2,193	885	30	34	14	21
19-1, 142	467.92	8,814	8,803	5,756	822	29	44	16	12
20-1, 121	505.71	25,954	4,145	3,902	761	65	22	7	5
20-2, 83	506.83	48,871	310	169	0	98	1	1	0
20-2, 90	506.90	26,460	655	406	0	98	1	1	0
20-2, 112	507.12	13,662	3,861	2,689	1,022	47	27	10	16
20-2, 119	507.19	3,124	1,755	1,397	246	35	36	16	13
20-3, 4	507.54	39,580	4,581	3,428	1,302	74	18	2	7
20-3, 14	507.64	7,108	2,064	1,799	377	47	29	12	11
20-3, 81	508.31	6,762	3,805	3,248	206	37	41	18	5
20-4, 123	510.23	1,850	1,806	1,996	352	26	34	23	18
21-3, 4	526.54	2,867	2,525	2,924	253	26	37	25	11
21-3, 36	526.86	7,193	2,829	2,714	308	42	34	17	8
21-3, 112	527.62	24,897	5,553	5,433	696	57	27	11	5
21-3, 125	527.75	7,030	2,890	2,647	200	43	37	16	5
21-3, 129	527.79	5,139	1,845	1,909	245	42	31	17	9
22-2, 67	554.17	3,034	1,640	1,451	251	35	34	17	13
22-2, 90	554.40	14,176	4,044	3,143	600	51	30	10	9
22-2, 110	554.60	6,362	886	618	568	53	18	7	21
22-3, 79	555.79	3,506	1,807	1,672	339	35	32	18	15
22-4, 49	556.99	6,263	2,589	2,954	367	38	32	20	11
23-3, 76	593.76	4,480	2,509	2,033	230	36	39	16	9
23-3, 100	594.00	3,608	377	207	574	47	15	9	30
23-4, 0	594.50	4,363	2,323	2,207	317	35	35	18	12
23-4, 43	594.93	32,485	2,266	1,639	1,916	68	12	2	17
24-2, 81	620.81	2,843	1,330	817	198	41	35	11	13
24-3, 18	621.68	11,855	3,299	1,891	373	57	33	5	6
24-3, 86	622.36	14,106	2,112	898	145	76	22	1	1
25-2, 109	649.59	4,054	558	245	295	59	19	4	19
25-3, 64	650.64	16,448	2,549	751	953	63	21	0	15
25-3, 121	651.21	6,448	1,365	567	591	51	23	6	21
25-6, 66	655.16	12,594	1,848	743	987	57	19	4	20
26-1, 27	666.27	13,665	3,354	877	118	65	33	1	1
26-1, 45	666.45	28,698	5,019	2,431	1,124	66	24	1	9
26-1, 109	667.09	6,920	422	260	0	96	3	1	0
26-2, 51	668.01	44,882	757	1,099	1,304	93	0	1	6
26-2, 61	668.11	41,131	409	492	0	98	1	1	0
26-2, 105	668.55	31,324	1,386	401	481	95	3	1	1
26-2, 130	668.80	35,873	5,221	764	962	75	21	1	3
27-1, 20	675.70	2,465	1,859	729	289	35	40	9	16
27-1, 51	676.01	13,076	3,633	723	279	63	35	1	1
27-1, 61	676.11	18,302	5,358	2,971	852	52	31	6	10

Table T8 (continued).

Core, section, interval (cm)	Depth (mbsf)	Clay mineral (wt%)*			Clay mineral (area%)†		
		Smectite	Illite	Chlorite	Smectite	Illite	Chlorite
31-297-							
15-2, 113	336.13	25	43	32	13	53	34
15-4, 85	338.85	20	48	31	9	58	32
16-2, 59	354.59	17	53	29	0	70	30
16-2, 130	355.30	32	49	19	2	83	15
16-3, 90	356.30	30	40	30	5	61	33
17-2, 9	392.09	20	49	31	6	62	32
17-2, 114	393.14	42	42	16	23	60	17
17-3, 10	393.60	25	42	33	2	61	37
17-3, 56	394.06	29	44	27	14	57	29
17-3, 118	394.68	25	43	32	3	62	35
18-1, 72	429.22	29	45	26	5	68	27
18-2, 88	430.88	22	52	26	5	68	27
18-2, 115	431.15	26	43	31	9	58	33
18-2, 133	431.33	38	44	18	18	63	19
19-1, 142	467.92	33	49	18	16	63	21
20-1, 121	505.71	69	23	7	52	33	16
20-2, 83	506.83	98	1	1	97	2	1
20-2, 90	506.90	98	1	1	89	9	3
20-2, 112	507.12	56	32	12	40	45	16
20-2, 119	507.19	40	41	18	24	54	22
20-3, 4	507.54	79	19	2	61	28	11
20-3, 14	507.64	53	33	14	37	44	19
20-3, 81	508.31	39	43	19	24	53	23
20-4, 123	510.23	31	41	28	14	55	31
21-3, 4	526.54	30	42	28	15	54	31
21-3, 36	526.86	45	37	18	30	47	23
21-3, 112	527.62	60	28	12	43	38	19
21-3, 125	527.75	45	39	17	29	48	22
21-3, 129	527.79	47	34	19	31	45	23
22-2, 67	554.17	41	40	20	24	52	23
22-2, 90	554.40	56	33	11	39	44	17
22-2, 110	554.60	68	23	9	57	32	11
22-3, 79	555.79	41	38	21	25	51	24
22-4, 49	556.99	42	36	22	28	46	26
23-3, 76	593.76	40	43	18	24	54	22
23-3, 100	594.00	66	21	13	65	27	7
23-4, 0	594.50	40	40	20	24	51	24
23-4, 43	594.93	83	15	2	72	20	7
24-2, 81	620.81	47	40	13	29	54	17
24-3, 18	621.68	60	35	5	41	46	13
24-3, 86	622.36	77	22	1	58	35	7
25-2, 109	649.59	72	23	5	60	33	7
25-3, 64	650.64	75	25	0	58	36	5
25-3, 121	651.21	64	29	8	49	42	9
25-6, 66	655.16	71	24	5	59	34	7
26-1, 27	666.27	66	33	1	47	47	6
26-1, 45	666.45	73	26	1	54	37	9
26-1, 109	667.09	96	3	1	76	18	6
26-2, 51	668.01	99	0	1	90	6	4
26-2, 61	668.11	98	1	1	94	4	2
26-2, 105	668.55	96	3	1	83	15	2
26-2, 130	668.80	77	22	1	62	36	3
27-1, 20	675.70	42	48	11	22	65	13
27-1, 51	676.01	64	35	1	45	50	5
27-1, 61	676.11	58	35	7	40	47	13

Table T8 (continued).

Core, section, interval (cm)	Depth (mbsf)	Bulk sample (wt%)*			Bulk sample (area%)†		
		Smectite	Illite	Chlorite	Smectite	Illite	Chlorite
31-297-							
15-2, 113	336.13	19	32	24	10	39	25
15-4, 85	338.85	15	35	23	7	43	24
16-2, 59	354.59	5	15	8	0	20	8
16-2, 130	355.30	14	21	8	1	36	6
16-3, 90	356.30	6	8	6	1	13	7
17-2, 9	392.09	6	14	9	2	18	9
17-2, 114	393.14	17	17	6	9	24	7
17-3, 10	393.60	6	11	8	1	15	9
17-3, 56	394.06	12	18	11	6	23	12
17-3, 118	394.68	4	7	6	0	11	6
18-1, 72	429.22	8	13	8	1	20	8
18-2, 88	430.88	14	33	16	3	43	17
18-2, 115	431.15	17	28	20	6	38	22
18-2, 133	431.33	12	13	5	5	19	6
19-1, 142	467.92	21	32	12	10	41	13
20-1, 121	505.71	50	17	5	37	24	11
20-2, 83	506.83	87	1	1	86	2	1
20-2, 90	506.90	91	1	1	82	8	3
20-2, 112	507.12	36	21	8	25	29	10
20-2, 119	507.19	21	22	10	13	28	11
20-3, 4	507.54	61	15	2	47	22	8
20-3, 14	507.64	40	25	10	28	33	14
20-3, 81	508.31	30	33	15	19	42	18
20-4, 123	510.23	24	31	21	11	42	23
21-3, 4	526.54	23	32	22	12	41	24
21-3, 36	526.86	33	27	14	22	35	17
21-3, 112	527.62	46	22	9	33	29	14
21-3, 125	527.75	35	30	13	23	38	18
21-3, 129	527.79	36	27	15	25	35	18
22-2, 67	554.17	21	20	10	12	27	12
22-2, 90	554.40						
22-2, 110	554.60	30	10	4	25	14	5
22-3, 79	555.79	29	27	15	18	36	17
22-4, 49	556.99	21	18	11	14	23	13
23-3, 76	593.76	32	35	14	20	44	18
23-3, 100	594.00	49	16	9	48	20	6
23-4, 0	594.50	29	29	15	18	38	18
23-4, 43	594.93	47	8	1	41	12	4
24-2, 81	620.81	34	29	9	21	40	12
24-3, 18	621.68	38	22	3	26	29	8
24-3, 86	622.36	58	17	1	43	26	6
25-2, 109	649.59	41	13	3	34	19	4
25-3, 64	650.64	56	19	0	44	27	4
25-3, 121	651.21	50	22	6	39	33	7
25-6, 66	655.16	51	17	4	42	25	5
26-1, 27	666.27	53	27	1	38	38	5
26-1, 45	666.45	39	14	1	29	20	5
26-1, 109	667.09	76	2	1	60	15	5
26-2, 51	668.01	88	0	1	80	5	4
26-2, 61	668.11	84	1	1	81	3	2
26-2, 105	668.55	83	3	1	72	13	2
26-2, 130	668.80	58	16	1	46	27	2
27-1, 20	675.70	28	32	7	15	45	9
27-1, 51	676.01	55	30	1	39	43	4
27-1, 61	676.11	40	24	5	28	32	9

Notes: * = SVD normalization factors. † = Biscaye (1965) normalization factors.